Primary cortical representation of sounds by the coordination of action-potential timing

R. Christopher deCharms & Michael M. Merzenich

Keck Center for Integrative Neuroscience, 828-HSE, University of California, San Francisco, California 94143, USA

Cortical population coding could in principle rely on either the mean rate of neuronal action potentials, or the relative timing of action potentials, or both. When a single sensory stimulus drives many neurons to fire at elevated rates, the spikes of these neurons become tightly synchronized[1,2], which could be involved in 'binding' together individual firing-rate feature representations into a unified object percept[3]. Here we demonstrate that the relative timing of cortical action potentials can signal stimulus features themselves, a function even more basic than feature grouping. Populations of neurons in the primary auditory cortex can coordinate the relative timing of their action potentials such that spikes occur closer together in time during continuous stimuli. In this way cortical neurons can signal stimuli even when their firing rates do not change. Population coding based on relative spike timing can systematically signal stimulus features, it is topographically mapped, and it follows the stimulus time course even where mean firing rate does not.

Although the timing[4–8] and correlations[9–13] of action potentials have been studied for over three decades, the fundamental logic of cortical population coding is still not understood. The firing rates of the majority of individual neurons in the primary auditory[14–16] somatosensory[17–19] and visual cortices[20,21] are changed most markedly only at the onset, offset, change or motion of a stimulus, and they typically habituate to nearer their background levels if the stimulus persists, with only a subgroup showing a markedly phasic–tonic profile. Further, it has recently been shown that sensorimotor neurons in the frontal cortex can change their relative timing during behaviour even when their mean firing rates are unchanged[22]. Are cortical neurons that fire at low rates uninvolved in signalling, or might they be signalling by some other mechanism at the level of the cortical population? Figure 1*f*,*g* shows the rate of individual action potentials recorded simultaneously from multiple neurons at each of two locations in the primary auditory cortex of an adult marmoset monkey, which were driven by a pure tone stimulus with the amplitude envelope shown in Fig. 1*e*, at a frequency appropriate to drive these two locations (4 kHz). Soon after the onset burst, the neurons returned to near their background firing rates, so the firing-rate response to a brief tone pulse (50 ms) was quite similar to that for an ongoing stimulus, although the two stimuli sound dramatically different.

The change in the pattern of relative timing between spikes from these same two locations during these stimuli is shown in Fig. 1*a*–*d*. We define the coordination of a population of neurons as the entire pattern of relative action-potential timing within that population, driven by both stimuli and internal dynamics, as this is the signal received by target populations. We define the coordinated rate of a single neuron or group of neurons as the rate of spikes that occur within a fixed time interval from a spike produced by a separate reference neuron or population of neurons. This is computed by making an average peristimulus time histogram of the rate of spikes from one location triggered on spikes from the other (Fig. 1*a*–*d*), and measuring the rate in a given bin. This measure reflects both relative timing and relative rate, which both affect postsynaptic targets. Each of the locations shown in Fig. 1 tended to fire more spikes that were close in time to a spike from the other location during the stimuli, even though the overall rate of spikes from each location was not increased, and the neurons were not phase locked to the stimulus (in cycle histograms, interval distributions, or shift predictors). In both cases, the change in coordinated rate was highly statistically significant ($P < 1 \times 10^{-5}$ for *b*, $P > 3 \times 10^{-4}$ for *c*; permutation test). As a control for changes in relative spike timing or short-term synaptic plasticity that might remain after a stimulus tran-

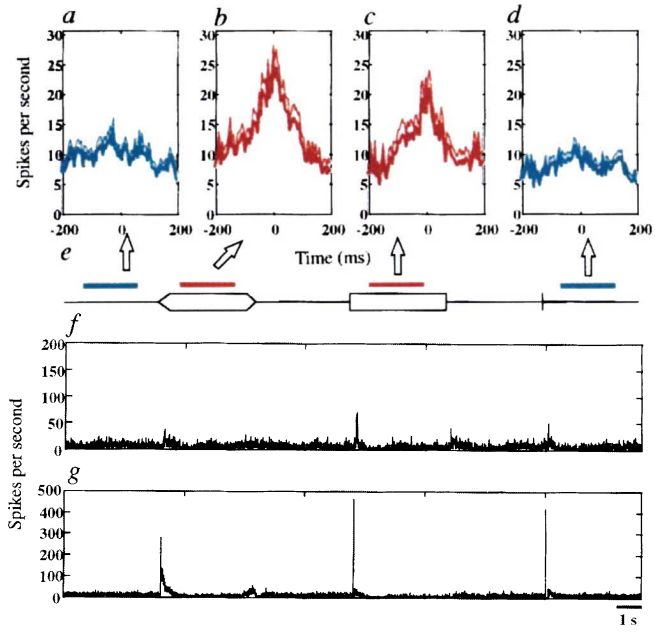

FIG. 1 Changes in mean firing rate and neuronal coordination in the primary auditory cortex during continuous pure-tone stimuli. A 4-kHz pure-tone stimulus with the amplitude envelope shown in *e* (maximum intensity 70 dB sound pressure level) was presented binaurally during multisite neuronal recording. Histograms of mean neuronal firing rates for two cortical locations are shown in *f* and *g*, and average cross-correlations between the two locations are shown in *a*–*d*, all constructed from 100 repetitions of the stimulus sequence. *a*–*d*, Rate of coordinated discharge (mean, thick line; mean plus standard error, thin line) between the two locations: *a*, during an initial silent period; *b*, during the 3-s constant phase of a ramped onset pure tone; *c*, during the same 3-s constant phase of a rapid onset pure tone; and *d*, during the silent period following the presentation of a 50-ms pure tone burst. *e*, Time periods for cross-correlation. The mean half-width at half-height of the central correlation peak in our sample was 11.2 ms (this example is particularly broad). Calculations excluded initial 500 ms after stimulus onsets, and were computed for individual trials by making a spike triggered average of the action-potential rate from the lower cortical location triggered on each action potential from the upper location, using 5 ms bins.

METHODS. We recorded neurons from pairs of locations in the supragranular primary auditory cortex of 3 marmoset monkeys anaesthetized using Nembutal, with electrode pairs separated by 75–1,000 μm. We used conventional sharp extracellular microelectrodes, standard electrophysiological amplification with filtering from 300 Hz to 10 kHz, computer storage of spike waveforms sampled at 20 kHz, and computer spike sorting. Data are from neuronal signals that were thresholded and sorted to remove non-neuronal waveforms, giving spike times from 54 pairs of single units with well-differentiated action potentials held throughout (Fig. 2), and 369 pairs of multiunit groups, which consist of the times of all individual action-potential waveforms recorded from each location. Auditory stimuli were generated by a DSP chip and presented binaurally using a closed speaker system. Values of statistical significance of differences between cross-correlograms were derived by calculating the cross-correlation for individual trials using 25-ms bins, which typically captured the central peak, and comparing the values at the zero phase-lag bin between different conditions using the permutation test (a Monte Carlo simulation that does not assume normal distribution)[27]. They were confirmed using the Mann-Whitney *U* test or joint peristimulus time histogram (JPST) analysis. Mean and s.e. values were derived from all trials, typically 100, and confidence limits were also computed using the point-wise bootstrap method[28]. We verified our results using two other normalization methods for correlograms: the raw number of coincidences (no normalization), or coincidences normalized by the auto-correlation of the spike trains interpolated to zero phase lag.

sient, we measured the coordinated rate immediately after a brief tone pulse that mimicked the stimulus onset (shown in *d*), and found it to be unchanged. Cortical neurons can thus maintain signals about ongoing stimuli by temporally coordinating the few action potentials present even at low firing rates.

To compare the patterns of coordination found between distinct pairs of individual neurons and within larger neuronal populations, we simultaneously recorded multiple isolated single neurons, multiunit clusters, and local field potentials. The coordinated rate histogram between two single neurons during silence and during a stimulus is shown in Fig. 2*a*. There appeared to be a stimulus-induced change, but there were far too few coordinated spikes at these low firing rates to have sufficient statistical power to measure the effect; this was true of nearly all single unit pairs. A pair of single neurons that did show a statistically significant increase in coordinated rate during the stimulus is shown in Fig. 2*b*, but the effect was still comparatively weak ($P < 0.04$). When we measured the change in average coordinated rate between all of the action potentials taken from two very small groups of neurons (each group containing one of the neurons shown in Fig. 2*b* and one additional cell), we found that the effect was very similar in form but was much more robust ($P < 0.018$). When we added all of the action potentials measured from these same two locations that were above a fixed size, the effect was stronger still ($P < 0.005$). The coordination between one of these single neurons and the local field potential, a measure of the global activity of all surrounding neurons, also showed a similar profile and a significant change ($P < 0.01$). The coordination between nearby pairs of neurons are often similar in form, so their effects can therefore summate and become much more robust in large populations than in single pairs.

Figure 3*a*–*h* illustrates the frequency tuning of spike time coordination from groups of neurons at two cortical locations that had traditional onset burst tuning to frequencies between 2 and 6 kHz. Groups of neurons from different locations were typically somewhat coordinated even during silence (Fig. 3*a*). Following a brief and frequency-tuned coordinated burst at stimulus onset, the neurons showed an enduring frequency-tuned change in coordinated rate throughout the stimulus (Fig. 3*b*–*h*). The coordinated rate of action potentials was significantly increased by a 4-kHz stimulus ($P < 0.05$; Fig. 3*e*), but significantly decreased by a 6.35-kHz stimulus ($P < 0.01$; Fig. 3*g*). The coordinated rate can increase even in cases where the overall mean firing rate is decreased (Fig. 3*e*; firing rate less than background, $P < 0.0001$). Where firing rate and relative timing both change, the absolute number of coordinated events reflects both effects.

A particular sound increases the coordinated rate within a restricted and tonotopically mapped sector of the cortical surface (Fig. 3, bottom; the spatial positions of pairs of cortical locations that increased their coordinated rate during the stimulus are connected by red lines, and those that decreased are connected by blue lines). The population response to a 4-kHz tone at 70 dB is shown in Fig. 3*i*, demonstrating that within a discrete subregion of the auditory cortex (containing about 10^6 neurons[23]), cells from almost all locations maintain a temporally coordinated pattern of spike timing after a widespread coordinated onset burst; this region may also be decorrelated from surrounding regions. A similar spatial pattern of spike-time coordination is maintained during a stimulus of the same frequency but 30 dB lower intensity (Fig. 3*j*). A stimulus with a nearby but different frequency (2.52 kHz), sampled at fewer points, coordinated a distinct but partly overlapping region (Fig. 3*k*). The centre frequency of coordinated spike tuning versus spatial location for pairs of locations from which we collected full coordination tuning curves is shown in Fig. 3*l*. Coordination tuning forms an organized topographic map across the cortical surface, commensurate with the map for traditional onset burst tuning.

Neuronal coordination could also mimic the time course of the stimulus for locations at which the firing rate did not. Two locations are shown in Fig. 4*b*, *c* that did not have any statistically significant change in firing rate in response to a long tonal stimulus, not even transients (because the stimulus rose so slowly; Fig. 4*d*), but still showed a tonic time course of coordinated discharge rate (Fig. 4*a*) that lasted throughout the stimulus. Figure 4*f* shows the sum of all of the firing-rate histograms for this stimulus from the population mapped in Fig. 3. Most of these locations produced a transient discharge, and some also showed smaller sustained changes in firing rate, but the mean of the individual firing rates was unchanged during the constant phase of the stimulus. In contrast, the mean of the coordinated firing-rate profiles from all of the pairs (Fig. 4*e*) showed an increase that lasted throughout the stimulus (Fig. 4*g*). This suggests that a target

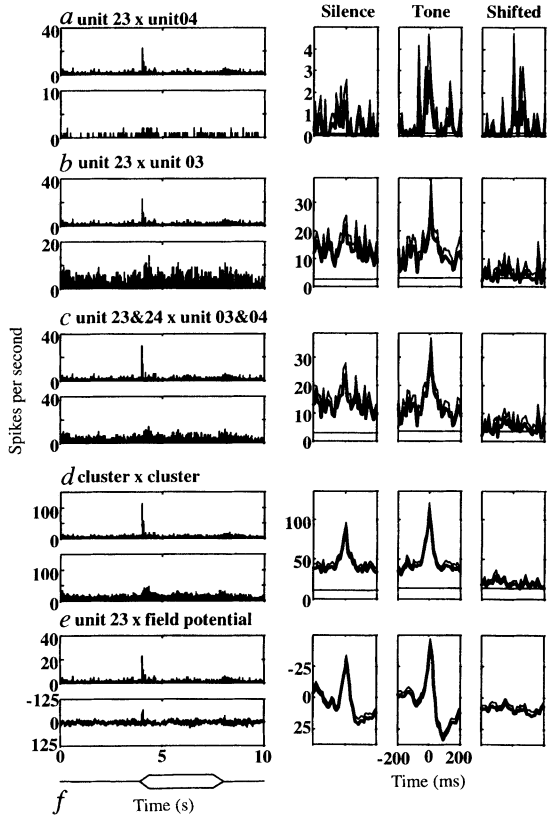

FIG. 2 Neuronal coordination is a population effect. Firing-rate responses from two locations (left: top, reference unit; bottom, target) and the coordination between the two (right) during the silence preceding a stimulus, and during the tonic phase of the stimulus. Far right, the 'shift predictor', a measure of the coordination between two locations that is locked to the timing of the stimulus, computed by making correlations between trial number n for the reference unit and trial $n + 1$ for the target unit. As we are interested in the total coordinated signal to a downstream target, whatever its source, we have not excluded stimulus-locked components using shift predictors of JPST analysis[29,30]. However, stimulus locking does not contribute to our measured correlation because we chose stimuli during which these neurons do not stimulus lock. None of the shift predictors showed significant stimulus-locked correlation. *a*, Two neurons that appear to increase their cross-correlation during a stimulus, but have too great a variability for the change to be reliably observed. *b*, Two neurons that did show a statistically significant change in cross-correlation due to the stimulus, but had little or no tonic change in firing rate. *c*, Correlation between two groups of well-isolated units, each comprising two neurons and including one of the units shown in *b*, which shows a very similar but more statistically robust effect. *d*, Correlation between two thresholded multiunit groups, which show a similar effect. *e*, Increase in correlation between a single unit and the local field potential recorded form an adjacent electrode (the voltage waveform filtered from 10 to 300 Hz to remove individual action potentials). *f*, Envelope of the presented 4-kHz, 70-dB stimulus. Field potentials are in μV. Mean, thick line; mean plus s.e., thin line.

location which samples across a broad and non-homogeneous population of neurons that are firing on average near background rate can nonetheless extract the time course of an ongoing stimulus by using temporal coincidence information from that population.

Coordinated relative spike timing could in principle be created by mechanisms of recurrent neural circuitry, by divergent temporal input to many neurons from a common internal source (possibly the thalamus in this case), or by divergent temporal input from a common external stimulus. All of these sources contribute to the signal received by a postsynaptic cell. Because neurons are temporal integrators, the synchronization and temporal pattern of

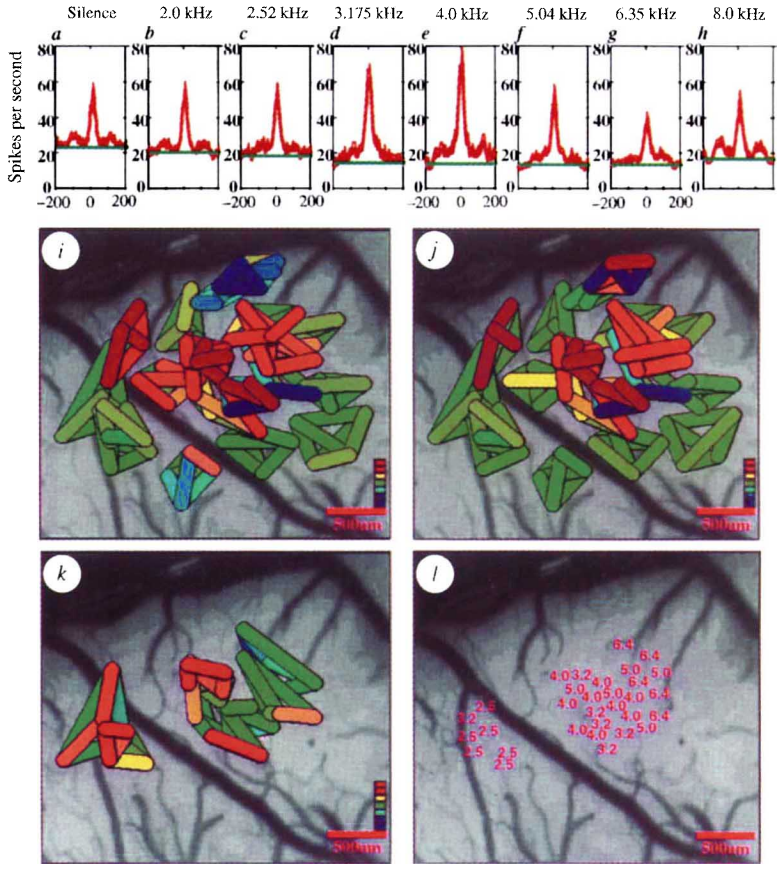

FIG. 3 Neuronal coordination is stimulus specific, and can be either increased or decreased relative to background by particular stimuli. *a–h*, Changes in cross-correlation between two locations during silence or 4-s, 70-dB, continuous pure-tone stimuli at different frequencies; mean, thick line; mean plus s.e., thin line. The green lines indicate the mean target-location firing rate during each period. All cross-correlations were computed (as described for Fig. 1) during the tonic phase of the stimulus, excluding onset and offset transient responses. Of 48 pairs of locations for which we constructed full coordination tuning curves using multiple stimuli, 90% showed a stimulus-dependent and frequency-tuned change in coordinated rate ($P < 0.05$ permutation test on central 25-ms bin: of these, 64% tuned increase, 15% tuned increase with surround decrease, 21% tuned decrease), and 10% showed no change. In every case the frequency tuning of ongoing spike coordination was commensurate with that observed for onset bursts, and in some cases was accompanied by changes in firing rate. Of 197 pairs for which we presented only a single stimulus frequency of 4 kHz, which was not the tuned frequency for some neurons, 39.3% showed a significant change in coordinated rate ($P < 0.05$, permutation test). Changes in neuronal coordination also generate an organized topographic map of sound frequency across the cortical surface. We recorded 96 locations in the primary auditory cortex of one monkey in groups of four, each group yielding six measures of cross-correlation, plotted as lines between the corresponding surface locations in *i–k*, with surface vasculature shown for spatial reference. Increases in coordinated rate during the stimulus are shown in red, decreases in blue. *i*, Cortical area that responded with a change in sustained coordination to a 4-kHz tone at 70 kB; *j*, responses of the same locations during presentation of the same tone at 40 dB; *k*, responses of a smaller number of locations during a 2.52-kHz tone at 40 dB; *l*, centre frequency of tonic phase coordinated discharge rate tuning for pairs of locations where a full tuning curve was computed, plotted near the midpoint of the line joining the two locations. Changes in coordination in *i–k* are plotted as the change in coordinated spike rate driven by the stimulus, divided by the background coordinated spike rate, $(C_{stim} - C_{back})/C_{back}$, with the order of overlaying of lines reflecting the magnitude of this index. The colour bar corresponds to index values of <-1, -1, -0.5, 0.05, 1, >1 from blue to red.

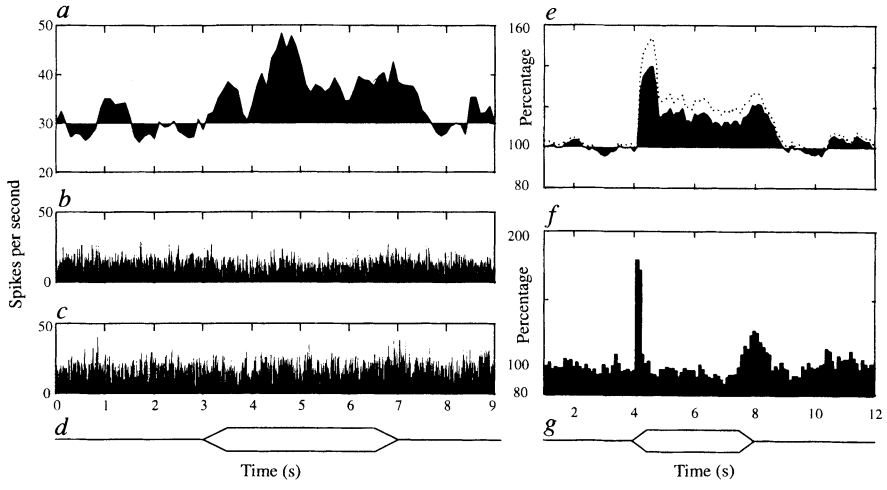

FIG. 4 Cortical sensory neurons can represent a stimulus and its time course through their coordination without any change in mean firing rate. *a*, Time course of the mean coordinated rate in a 500-ms time window ending at the time plotted; *b*, *c*, histograms (binned to 5 ms) of the evoked firing rates of the neurons at the two cortical locations summed over 100 stimulus presentations; *d*, time course of the stimulus envelope of the 4-kHz, 70-dB tonal stimulus. The coordinated spike rate was computed by calculating the average rate of target-location spikes in a 25-ms bin centred on all reference location spikes during a 500-ms segment of the trial (using the spike-triggered average method as before). Subsequent points in *a* are shifted by 100 ms, leading to 5 × 'oversampling', and shading is centred around the background period mean. The time courses of firing rate and coordinated firing rate were computed for all pairs of locations for this stimulus, and each was normalized to its own background rate. *e*, Mean plus standard error of all coordinated spike-rate time courses, each expressed as a percentage of its own baseline rate. The dotted line indicates the mean plus standard error of all of the curves. *f*, Average of all of the individual firing rates for the same locations, also expressed as a percentage of baseline rate and binned a 100 ms. The population mean of the coordinated discharge rate remains elevated throughout the time course of a long stimulus (in *g*), while the population mean of individual firing rates marks only the stimulus transients.

inputs arriving at a target cell can, in principle, be used to increase or decrease its output according to basic properties of synaptic integration[24–26]. At stimulus transients, spikes are necessarily coordinated, so population firing rate and coordinated firing rate reflect essentially the same phenomenon, and these two sides of population signalling presumably work together to provide robust cortical signals in many circumstances. Our results demonstrate that the relative spike timing of cortical action potentials may be a fundamental mechanism for signalling basic object features, one that goes well beyond neuronal grouping. They suggest that a basic cortical signal may be the number of temporally coordinated action potentials in a large neuronal population, which could converge to drive target neurons. Our data can also be understood as a reflection of the temporal patterns of activity that evolve moment by moment in cortical circuitry.

Note added in proof: We have recently observed similar phenomena both in the awake animal and in the primary somatosensory cortex. □

Received 5 September 1995; accepted 16 April 1996.

1. Gray, C. M., Konig, P., Engel, A. K. & Singer, W. *Nature* **338,** 334–337 (1989).
2. Singer, W. & Gray, C. M. *A. Rev. Neurosci.* **18,** 555–586 (1995).
3. von der Malsburg, C. Internal report, Max Planck Institute for Biophysical Chemistry, Gottingen, Germany (1981).
4. Adrian, E. D. *Electroenceph. clin. Neurophysiol.* **2,** 377–388 (1950).
5. Perkel, D. H., Gerstein, G. L. & Moore, L. *Biophys. J.* **7,** 391–418 (1967).
6. Middlebrooks, J. C., Clock, A. E., Xu, L. & Green, D. M. *Science* **264,** 842–844 (1994).
7. Abeles, M., Bergman, H., Margalit, E. & Vaadia, E. *J. Neurophysiol.* **70,** 1629–1638 (1993).
8. Abeles, M. *Corticonics: Neural Circuits of the Cerebral Cortex* (Cambridge Univ. Press, New York, 1991).
9. Dickson, J. W. & Gerstein, G. L. *J. Neurophysiol.* **37,** 1239–1261 (1974).
10. Eggermont, J. J. *J. Neurophysiol.* **71,** 246–270 (1994).
11. Ts'o, D. Y., Gilbert, C. D. & Wiesel, T. N. *J. Neurosci.* **6**(4), 1160–1170 (1986).
12. Ahissar, M. *et al. J. Neurophysiol.* **67,** 203–215 (1992).
13. Nicolelis, M. A. L., Baccala, L. A., Lin, R. C. S. & Chapin, J. K. *Science* **268,** 1353–1358 (1995).
14. Brugge, J. F. & Merzenich, M. M. *J. Neurophysiol.* **36,** 1138–1158 (1973).
15. Creutzfeldt, O., Hellweg, F. C. & Schreiner, C. *Expl Brain Res.* **39,** 87–104 (1980).
16. Pfingst, B. E. & O'Connor, T. A. *J. Neurophysiol.* **45,** 16–34 (1981).
17. Mountcastle, V. B., Davies, P. W. & Berman, A. L. *J. Neurophysiol.* **20,** 374–407 (1957).
18. Mountcastle, V. B. *J. Neurophysiol.* **20,** 408–434 (1957).
19. Mountcastle, V. B., Talbot, W. H., Sakata, H. & Hyvarinen, J. *J. Neurophysiol.* **32,** 452–484 (1969).
20. Hubel, D. H. & Wiesel, T. N. *J. Physiol. Lond.* **160,** 106–154 (1962).
21. Maunsell, J. H. R. & Gibson, J. R. N. *J. Neurophysiol.* **68,** 1332–1344 (1992).
22. Vaadia, E. *et al. Nature* **373,** 515–518 (1995).
23. Gabbot, P. L. A. & Stewart, M. G. *Neuroscience* **21,** 833–845 (1987).
24. Grannam, E. R., Kleinfeld, D. & Sompolinsky, H. *Neural. Computat.* **5,** 550–569 (1993).
25. Murthy, V. N. & Fetz, E. E. *Neural Comput.* **6,** 1111–1126 (1994).
26. Bernander, O., Koch, C. & Usher, M. *Neural Computat.* **6,** 622–641 (1994).
27. Lehmann, E. L. *Nonparametrics: Statistical Methods Based on Ranks* (Holden-Day, San Francisco 1975).
28. Efron, B. *The Jackknife, The Bootstrap, and Other Resampling Plans* 75–87 (Society for Industrial and Applied Mathematics, Philadelphia, 1982).
29. Perkel, D. H., Gerstein, G. L. & Moore, G. P. *Biophys. J.* **7,** 419–440 (1967).
30. Aertsen, A. M., Gerstein, G. L., Habib, M. K. & Palm, G. *J. Neurophysiol* **61,** 900–917 (1989).

ACKNOWLEDGEMENTS. We thank M. Fong, X. Wang, P. Bedenbaugh and D. Buonomano for technical and experimental assistance; E. Ahissar, W. Bialek, D. Ferster, D. Kleinfeld, W. Newsome, W. Singer and others for comments on the manuscript; and K. Parker and J. Stevens for outstanding scientific training. This work was supported by the NIH and by an NSF graduate fellowship to C.d.C.

CORRESPONDENCE and requests for materials should be addressed to M.M.M. (e-mail: merz@phy.ucsf.edu).

Absence of spectrally specific lateral inputs to midget ganglion cells in primate retina

David J. Calkins* & Peter Sterling

Department of Neuroscience, University of Pennsylvania, Philadelphia, Pennsylvania 19104, USA

Visual information is conveyed to the brain by retinal ganglion cells. Midget ganglion cells serve fine spatial vision[1,2] by summing excitation from a receptive field 'centre', receiving input from a single cone in the central retina, with lateral inhibition from a receptive field 'surround', receiving input from many surrounding cones. Midget ganglion cells are also thought to serve colour opponent vision[1–6] because the centre excitation is from a cone of one spectral type, while the surround inhibition is from cones of the other type[4,6]. The two major cone types, middle(M)- and long-(L)wavelength sensitive, are equally numerous and randomly distributed in the primate central retina[7–9], so a spectrally homogeneous surround requires that the cells mediating lateral interactions (horizontal or amacrine cells) receive selective input from only one cone type. Horizontal cells cannot do this because they receive input indiscriminately from M and L cones[10–12]. Here we report that the amacrine cells connected to midget ganglion cells are similarly indiscriminate. The absence of spectral specificity in the inhibitory wiring raises doubt about the involvement of midget ganglion cells in colour vision and suggests that colour opponency may instead be conveyed by a different type of ganglion cell.

Amacrine cells extend laterally fine processes (~0.1 μm in diameter) interrupted by varicosities (~0.5–2.0 μm in diameter) containing synaptic vesicles (Fig. 1). The varicosities are the main sites of excitatory input from bipolar cells and inhibitory output to bipolar and ganglion cells[13]. However, whether the varicosities excited by one midget bipolar cell direct their synapses to the same or to neighbouring midget circuits was unknown (but see refs 5,13). We sought the answer by identifying the amacrine cell processes presynaptic to a midget ganglion cell and its midget bipolar cell, and then tracing them through serial sections to identify their bipolar cell inputs.

A midget ganglion cell dendrite postsynaptic to its midget bipolar cell and surrounded by amacrine cell varicosities (A_{1-9}) is shown in Fig. 1. Two of these varicosities (A_1 and A_8) are postsynaptic to the bipolar cell; A_1 is also presynaptic to the ganglion cell, while A_8 is presynaptic to the bipolar cell. Most varicosities postsynaptic to a particular midget bipolar cell were seen to feed back to the same cell (77%), feed forward to the midget ganglion cell (63%), or do both (53%). Conversely, amacrine cell processes contacting a midget bipolar cell or its ganglion cell (for example, A_2) were usually postsynaptic to the very same bipolar cell (Fig. 1 legend). Thus, for most of the amacrine cell processes associated with midget circuits ('on' as well as 'off'), inputs and outputs are at the same bipolar cell and therefore cannot be spectrally antagonistic.

We next investigated whether there could be cone-selective inputs to other regions of the amacrine cell. We traced and reconstructed three neighbouring amacrine cells (Fig. 2). These cells, although possibly incomplete (and therefore of uncertain type), span and mingle with a patch of 15 midget bipolar cells. A fourth amacrine cell arbor was also reconstructed and spanned a patch of four midget bipolar cells (Fig. 2). The midget bipolar cell array reflects faithfully the cone array, as cone axons do not cross each other[11], and neither do midget bipolar cell axons[8]. Thus, we could determine whether inputs to four amacrine cells from a field of 19 midget bipolar cells showed any selectivity. This region also contained terminals from at least five diffuse bipolar cells. These cells collect non-selectively from both M and L cones[14], so it was important to discover whether they also contact the amacrine cells.

Each amacrine cell collected from all the bipolar cells within its reach. Thus, cell 1 received 20 synapses from 10 midget bipolar

* Present address: Max Planck Institute for Brain Research, Deutschordenstrasse 46, D-60528 Frankfurt, Germany.